Nanoscale

Accepted Manuscript

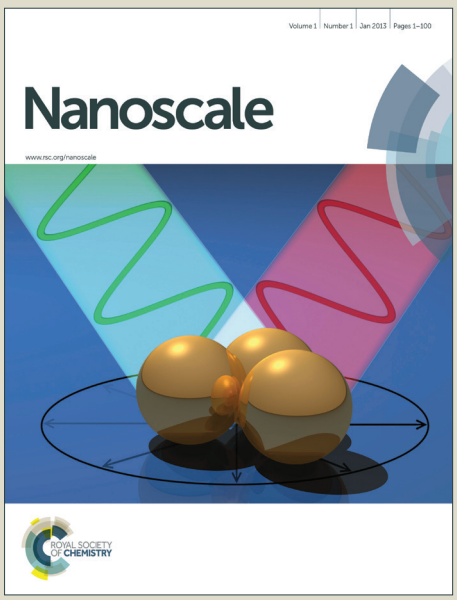

ROYAL SOCIETY OF CHEMISTRY

www.rsc.org/nanoscale

Nanoscale

RSCPublishing

ARTICLE

Multifunctional Non-viral Gene Vectors with Enhanced Stability, Improved Cellular and Nuclear Uptake Capability, and Increased Transfection Efficiency

Cite this: DOI: 10.1039/xoxxoooooox

Received ooth,
Accepted ooth

DOI: 10.1039/xoxxoooooox

www.rsc.org/

Zhe Yang[a], Zhaozhong Jiang[b], Zhong Cao[a], Chao Zhang[a], Di Gao[a], Xingen Luo[a], Xiaofang Zhang[a], Huiyan Luo[a,c], Qing Jiang[a], Jie Liu[a,*]

We have developed a new multifunctional, non-viral gene delivery platform consisting of cationic poly(amine-*co*-ester) (PPMS) for DNA condensation, PEG shell for nanoparticle stabilization, poly(γ-glutamic acid) (γ-PGA) and mTAT (a cell-penetrating peptide) for accelerated cellular uptake, and a nuclear localization signal peptide (NLS) for enhanced intracellular transport of DNA to the nucleus. *In vitro* study showed that coating of the binary PPMS/DNA polyplex with γ-PGA promotes cellular uptake of the polyplex particles particularly by γ-glutamyl transpeptidase (GGT) -positive cells due to GGT-mediated endocytosis pathway. Conjugating PEG to the γ-PGA led to the formation of the ternary PPMS/DNA/PGA-*g*-PEG polyplex with decreased positive charges on the surface of the polyplex particles and substantially higher stability in serum-containing aqueous medium. The cellular uptake rate was further improved by incorporating mTAT into the ternary polyplex system. Addition of NLS peptide was designed to facilitate intracellular delivery of the plasmid to the nucleus-a rate-limiting step in gene transfection process. As the result, compared with the binary PPMS/LucDNA polyplex, the new mTAT-quaternary PPMS/LucDNA/NLS/PGA-*g*-PEG-mTAT system exhibited reduced cytotoxicity, remarkably faster cellular uptake rate, and enhanced transport of DNA to the nucleus. All these advantageous functionalities contribute to the remarkable gene transfection efficiency of the mTAT-quaternary polyplex both *in vitro* and *in vivo*, which exceeds that of the binary polyplex and commercial Lipofectamine™ 2000/DNA lipoplex. The multifunctional mTAT-quaternary polyplex system with improved efficiency and reduced cytotoxicity represents a new type of promising non-viral vectors for delivery of therapeutic genes to treat tumors.

Introduction

Gene therapy has great potential to treat genetic disorders including cancers.[1,2] Because naked nucleic acids are susceptible to degradation *in vitro* or *in vivo*, gene vectors are required to achieve effective gene therapeutic treatments.[3] In the past, both viral and non-viral vectors have been employed for gene delivery.[4] Compared with viral gene vectors, non-viral gene vectors generally are safer, easier to produce at a low cost, and can be multifunctional via rational design and modification.[5] One important type of non-viral gene vectors are synthetic cationic polymers that are capable of condensing DNA to form nanosized polyplexes. Examples of such polymers include poly(ethyleneimine) and its derivatives,[6] poly(4-hydroxy-L-proline ester) (PHP), poly(α-(4-aminobutyl)-L-glycolic acid) (PAGA), poly(amine-*co*-esters),[7] poly(β-amino esters) (PBAE), poly(L-lysine) (PLL),[8] chitosan, poly(dimethylaminoethyl methacrylate), and poly(trimethyl-aminoethyl methacrylate). Among these materials, poly(amine-*co*-esters) are particularly promising due to their biodegradability, low cytotoxicity, and outstanding transfection efficacy.[9-11] Nevertheless, substantial challenges still remain in using polyplexes for gene delivery, especially for *in vivo* delivery applications. The limitations on many existing polyplex systems are excessive positive charges on the surface of polyplex particles, high toxicity, low *in vivo* stability,[12] relatively low cellular uptake rate, and impeded intracellular transport of plasmid into the nucleus.[13] Thus, it is anticipated that the efficiency of the gene vectors can be markedly improved when all these gene delivery barriers are overcome successfully.

To achieve maximal gene delivery efficiency, we have

developed following strategies to impart high stability, reduced toxicity, and enhanced cellular and nuclear uptake capability for polyplex particles. First, poly(γ-glutamic acid)-poly(ethylene glycol) graft copolymer (γ-PGA-*g*-PEG) was synthesized and employed to coat polyplexes via electrostatic interactions to reduce their excessive positive surface charges, to minimize their toxicity, and to increase the particle stability in aqueous medium. Compared with other anionic polymers such as hyaluronic acid (HA)[14] and oligonucleotides,[15] γ-PGA is more attractive due to its desirable biological properties including nontoxicity, excellent biocompatibility and minimal immunogenicity.[16-18] Additionally, γ-PGA is recognizable by γ-glutamyl transpeptidase (GGT, an intrinsic membrane protein) in GTT-positive cells, and nanoparticles coated with γ-PGA can possess remarkably accelerated cellular uptake rate.[19,20] Thus, in such cases, γ-PGA coating on cationic polyplexes is effective to lower the polyplex toxicity without decreasing their cellular uptake efficiency.[19,21] Secondly, a modified HIV-1 Tat (mTAT) was produced by covalently fusing the original Tat peptide with 10 histidine residues to serve as a cell-penetrating peptide. mTAT was subsequently conjugated to the γ-PGA-*g*-PEG to form γ-PGA-*g*-PEG-mTAT coating for further facilitating the cellular internalization and endosomal escape of polyplex particles.[22] Lastly, to overcome a major barrier in gene transfection, a cationic nuclear localization signal peptide (NLS) was added to electrostatically bind to DNA in polyplex particles to promote intracellular transport of DNA load to the nucleus.[23,24] NLS peptides can be recognized by nuclear transport protein to allow active nuclear uptake of NLS-bound DNA.

In this article, we wish to report a multifunctional, non-viral gene delivery platform developed on the basis of the above design strategies, which consist of cationic poly(ω-pentadecalactone-*co*-*N*-methyldiethyleneamine-*co*-sebacate) (PPMS) for DNA condensation to form polyplex nanoparticles, PEG shell for nanoparticle stabilization, γ-PGA and mTAT for accelerated cellular uptake, and NLS for enhanced intracellular transport of DNA to the nucleus (Scheme 1). As reported in our previous work, PPMS copolymers with 10-20% ω-pentadecalactone (PDL) were highly efficient gene vectors in transfecting various cell lines, but their unmodified polyplexes with DNA were not sufficiently stable for systemic *in vivo* gene delivery.[12] Compared with the binary PPMS/DNA polyplex, the newly constructed multifunctional polyplex PPMS/DNA/NLS/PGA-*g*-PEG-mTAT (mTAT-quaternary polyplex) indeed exhibited substantially higher stability, reduced cytotoxicity, faster cellular uptake rate, and enhanced capability of transporting DNA to the nucleus. The composition-dependent physicochemical properties of the mTAT-quaternary system were investigated and the gene transfection efficiency of the polyplex system was optimized.

Experimental

Materials

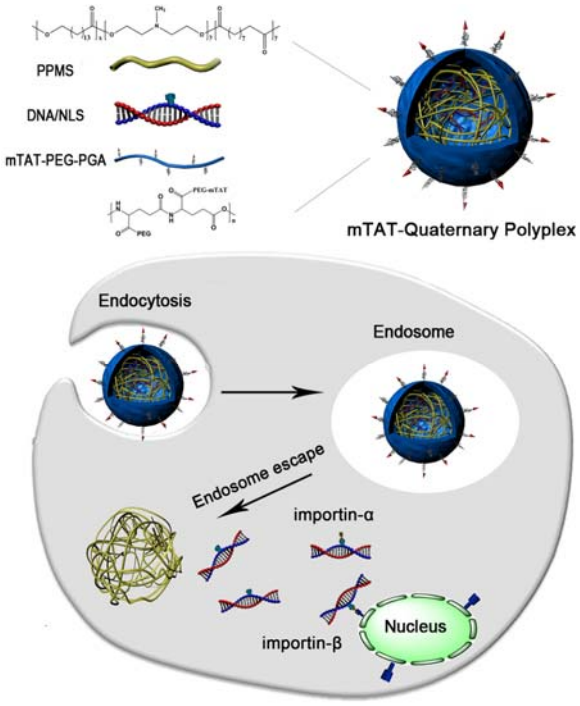

Scheme 1. Schematic diagram illustrating assembly of mTAT-quaternary polyplex particles, their cellular uptake, and intracellular delivery to the nucleus.

ω-Pentadecalactone (PDL), diethyl sebacate (DES), *N*-methyldiethanolamine (MDEA) and diphenyl ether were purchased from Aldrich Chemical Co. in the highest available purity and were used as received. Immobilized *Candida antarctica* lipase B (CALB) supported on acrylic resin or Novozym 435 was also obtained from Aldrich Chemical Co. and was dried at 50 °C under 2.0 mmHg for 20 h prior to use. Poly(γ-glutamic acid) (γ-PGA, 5000 Da) was purchased from Nanjing Sai Taisi Biotechnology Co. Ltd. (China). MeO-poly(ethylene glycol)-NH_2 (mPEG-NH_2, 3000 Da) and maleimide-poly(ethylene glycol)-NH_2 (Mal-PEG-NH_2, 3500 Da) was purchased from Jenkem Technology Co. Ltd. (China). NLS (PKKKRKV) and mTAT (CHHHHHRKKRRQRRRRHHHHHC) were synthesized by China Peptides Co. Ltd. Hoechst 33342 and 3-(4,5-dimethyl-2-thiazolyl)-2,5-diphenyl-2H-tetrazolium bromide (MTT) were obtained from Sigma. Gel red was purchased from Biotium Inc. (USA). Micro-BCA protein assay was obtained from Thermo Fisher Scientific Inc. *Label* IT® Tracker™ Intracellular Nucleic Acid Localization Kit was purchased from Mirus (Madison, WI). Lipofectamine™ 2000 (LF2K) was purchased from Invitrogen™. Reporter Lysis 5X Buffer and Luciferase Assay Buffer were obtained from Promega Co. (Madison, WI). Mouse TNF-related apoptosis-inducing ligand (TRAIL) was purchased from Abcam (Cambridge, MA). ECL kit was bought from Applygen Technologies Inc. (China). Antibody horseradish peroxidase (HRP)-labeled goat anti-mouse secondary antibody was used for Western blot. HepG2 cells, Hela cells and CT-26 cells were acquired from Shanghai cell bank of Chinese

Academy of Science (Shanghai, China) and were maintained in DMEM (Hyclone) containing 10% (v/v) fetal bovine serum (FBS) and 1% (w/v) penicillin-streptomycin at 37 °C under a 5% CO_2 humidified atmosphere.

Synthesis of PGA-*g*-mPEG and PGA-*g*-PEG-mTAT

Poly(glutamic acid)-graft-poly(ethylene glycol) (PGA-*g*-mPEG) was prepared according to the method reported in literature.[25] Briefly, poly(γ-glutamic acid) (γ-PGA, 5000 Da), *N*-hydroxysuccinimide (NHS) and MeO-poly(ethylene glycol)-NH_2 (mPEG-NH_2, 3000 Da) in different ratios were co-dissolved in borate saline buffer (0.05 M, pH = 8.5). The resultant solution was mixed with *N*-(3-dimethylaminopropyl)-*N*′-ethylcarbodiimide hydrochloride crystallite (EDC) and the whole mixture was stirred at room temperature for 6 h. Subsequently, the mixture was dialyzed (MWCO 5,000 Da) against deionized water for 24 h. The obtained product was freeze-dried and stored at -20 ºC. The proton NMR spectrum of the conjugate showed the characteristic resonance of mPEG at 3.3 ppm (-OCH_3) and the absorption of PGA at 2.3 ppm (-CH_2CH_2COO-) (Figure S1 A). The grafting percentage of PGA-*g*-mPEG is determined based on the proton resonance absorptions and calculated as the percentage of PGA carboxylate groups that are PEGylated.

The procedure for synthesis of PGA-*g*-PEG-mTAT was analogous to that used for preparation of PGA-*g*-mPEG as described above. Briefly, the γ-PGA was conjugated to the terminal amino group of Mal-PEG-NH_2. The resultant PGA-*g*-PEG-Mal was subsequently reacted with mTAT overnight at 4 ºC in PBS (pH = 7.0) containing 0.5 M EDTA to form PGA-*g*-PEG-mTAT. The molecular structure of PGA-*g*-PEG-mTAT was confirmed by proton NMR spectroscopy showing the characteristic resonance of mTAT at 7.13 ppm (-NH-*CH*=N-) and the resonance absorption of PGA at 4.13 ppm (-NHC*H*CO-) (Figure S1 B). The percentage of the PEG blocks conjugated to mTAT is calculated on the basis of the proton absorptions and is designated as % mTAT to describe mTAT content in PGA-*g*-PEG-mTAT.

Preparation of multiple component polyplexes

DNA/PPMS/PGA-*g*-mPEG ternary polyplexes, DNA/PPMS/γ-PGA ternary polyplexes, and DNA/NLS/PPMS/PGA-*g*-PEG-mTAT quaternary polyplexes were prepared according to following procedures. The N/P/C ratio used represents the molar ratio of the amino groups in PPMS to the phosphate groups in DNA to the carboxyl groups in γ-PGA or PGA-*g*-mPEG. Typically, plasmid DNA was mixed with PPMS solution in NaAc (25 mM, pH=5.2) at N/P ratio of 150 to form DNA/PPMS binary polyplex. After 30 min incubation, PGA-*g*-mPEG or γ-PGA was added to the binary polyplex at different N/C ratios and the resultant mixture was thoroughly blended by pipetting and sequentially incubating at room temperature for 30 min to generate DNA/PPMS/PGA-*g*-mPEG or DNA/PPMS/γ-PGA ternary polyplexes. The DNA/NLS/PPMS/PGA-*g*-PEG-mTAT quaternary polyplexes were fabricated using similar procedures as those employed for the ternary polyplex preparation except that in the first step, DNA/NLS mixture was used instead of DNA to form DNA/NLS/PPMS polyplexes and in the second step, (PGA-*g*-PEG-mTAT)/(PGA-*g*-mPEG) at different ratios were used instead of PGA-*g*-mPEG for surface coating.

Characterization of polyplex size, zeta potential and morphology

The size distribution and zeta potential of polyplexes in aqueous suspension were measured by dynamic light scattering (DLS) using Malvern Zetasizer Nano ZS90, and all measurements were performed at 25 °C. The morphology of polyplexes was analyzed using a Transmission Electron Microscope (JEM 1400). The samples were dropped on a copper grid and negatively stained by aqueous solution of uranyl acetate to observe the morphology.

Dye exclusion assay

The DNA condensation capability of polyplexes was determined by performing gel red exclusion assay as reported previously.[26] During the experiment, an aliquot of 100× gel red solution was added to a polyplex solution or a naked DNA solution containing the same amount of DNA, and the resultant mixture was incubated at room temperature in dark for 10 min. The fluorescence intensity of the mixture was measured using a microplate reader (BioTek Synergy4) at excitation and emission wavelengths of 510 and 590 nm, respectively. The relative fluorescence intensity of polyplex samples was calculated using the following equation.

$$\text{Relative Fluorescence (\%)}=\frac{(F_{\text{Sample}}-F_{\text{Gel Red}})}{(F_{\text{DNA}}-F_{\text{Gel Red}})}\times 100\%$$

Where F_{Sample}, F_{DNA} and $F_{\text{Gel Red}}$ represent the fluorescence intensity values of polyplex sample, naked DNA and gel red, respectively.

Polyplex stability studies

Stability of polyplex samples were evaluated by monitoring the size change of polyplex particles under mimic physiological conditions *in vitro*. Typically, polyplex samples were incubated in PBS solution (0.01 M, pH = 7.4) containing 10% FBS and were gently stirred at 37 °C. At various time intervals, 100 μL aliquots were withdrawn from the polyplex solutions to measure the polyplex particle sizes using DLS. All measurements were performed in triplicate.

In vitro gene transfection studies

Effects of γ-PGA on gene transfection efficiency

The influence of γ-PGA coating on transfection efficiency of luciferase gene (LucDNA)-loaded binary and ternary polyplexes were carried out at various N/C molar ratios against

HepG2 cells (GGT positive cell line) and Hela cells (GGT negative cell line).[27] Briefly, HepG2 cells or Hela cells were seeded in a 24-well plate at a density of 7.5×10^4 cells/well and were incubated in DMEM medium (500 μL/well) with 10% FBS at 37 °C in 5% CO_2 atmosphere. After allowing the cells to adhere overnight, the polyplexes containing 1 μg of LucDNA were added into each well. LF2K/LucDNA lipoplex was used as the positive control. All transfection experiments were performed in triplicate. After 6 h incubation, the transfection media were removed and were replaced by fresh DMEM containing 10% FBS. The cells were further incubated for 42 h. For luciferase assay, the medium was aspirated and cells were rinsed twice by PBS. Subsequently, the cells were lysised in 200 μL of 1× reporter lysis buffer (Promega). After the cell lysate was transferred into an eppendorf tube and centrifuged at 12,000 rpm for 10 min, the supernatant (20 μL) was mixed with luciferase assay buffer (100 μL) and the fluorescence intensity (in terms of relative light units or RLU) were measured with a luminometer (Promega). The protein content in the supernatant was determined using BCA protein assay kit (Pierce, USA) and gene transfection efficiency is calculated as RLU/mg protein. For competitive inhibition experiments, HepG2 cells were incubated with polyplexes in DMEM medium additionally containing 10 μM or 20 μM of free γ-PGA. After 6 h incubation, the transfection medium was replaced with fresh DMEM medium and cells were incubated for another 42 h at 37 °C. The luciferase gene transfection efficiency of the polyplex samples was determined according to the procedures described above.

Optimization of the DNA/NLS/PPMS/PGA-g-PEG-mTAT quaternary polyplexes

To optimize the formulation of the quaternary polyplexes, the N/C ratio of PPMS/DNA/γ-PGA ternary polyplexes, the NLS/DNA ratio and PGA-*g*-PEG-mTAT blending ratio of the quaternary polyplexes were varied to determine their effects on luciferase transfection efficiency in HepG2 cells. Briefly, HepG2 cells were seeded in a 24-well plate at a density of 7.5×10^4 cells/well and were incubated in DMEM medium (500 μL/well) with 10% FBS at 37 °C in 5% CO_2 atmosphere. After allowing the cells to adhere overnight, the different polyplex formulations containing 1 μg of luciferase plasmid were added into each well and were cultured with cells for 48 h. All transfection experiments were performed in triplicate. At the end of incubation, the culture medium was removed and the cells were washed twice with PBS solution. The luciferase expression efficiency was quantified using the same procedures as described above in section "Effects of γ-PGA on gene transfection efficiency".

Green fluorescent protein assay

The efficiency of the multi-component polyplexes in transfecting EGFP reporter gene was also investigated using HepG2 cells. The experimental procedures were similar to those used for performing luciferase gene transfection as described in section "Effects of γ-PGA on gene transfection efficiency". After treatment of the cells with polyplexes containing EGFP plasmid for 48 h, the fluorescence intensity of EGFP-expressed protein in HepG2 cells was quantified using FACSCallibur (Becton Dickinson, San Jose) at excitation wavelength of 488 nm. Data collection involved 10,000 counts per sample. LF2K/EGFP lipoplex was employed as a positive control in this study on EGFP gene transfection.

The cytotoxicity of report gene-loaded polyplexes

HepG2 cells were employed to evaluate the cytotoxicity of different LucDNA-loaded polyplex formulations by MTT assay. Cells were seeded in a 96-well plate at a density of 1×10^4 cells/well and were cultured for 24 h in DMEM (200 μL/well) containing 10% FBS in a humidified atmosphere with 5% CO_2. Thereafter, the cells were incubated with the polyplex samples at various concentrations for 48 h. At the end of the incubation period, the culture medium was removed and the cells were rinsed three times with PBS solution (0.01 M, pH = 7.4). Subsequently, 100 μL of fresh medium and 20 μL of PBS containing 5 mg/mL of MTT were added to each well and the cells were incubated at 37 °C for additional 4 h. After removal of the medium, the resultant formazan salt crystals were dissolved in DMSO and were quantitatively measured using a microplate reader (BioTek Synergy 4) at the absorption wavelength of 570 nm. All assays were carried out in triplicate.

Erythrocyte agglutination and hemolysis assay

Erythrocytes were isolated by centrifugation of human blood at 2,500 rpm for 5 min and were washed three times in 0.9% NaCl aqueous solution at 4 °C. A stock suspension of the erythrocytes at a density of 2×10^6 cells/mL was prepared for erythrocyte agglutination study. An equal volume mixture of the erythrocyte suspension and polyplex solution containing 250 μg/mL polymer was incubated at 37 °C for 1 h. At the end of the incubation period, 10 μL of the solution mixture was spread on a glass plate to examine erythrocyte agglutination by a microscope. For hemolysis study, polyplex samples with various concentrations were mixed with the erythrocytes suspension (1×10^8 cells/mL) and the resultant mixtures were incubated at 37 °C for 1 h. After incubation, the erythrocytes-containing mixtures were centrifuged at 1,500 rpm for 5 min, and the supernatants were isolated. Hemolysis was quantified by measuring the absorbance of hemoglobin in the supernatants at a wavelength of 410 nm using a microplate reader (BioTek Synergy4). Triton X-100 (0.1%, w/v) and isotonic NaCl solution were used as positive control and negative control, respectively. The results are reported as percentage hemolysis with the assumption that Triton X-100 and NaCl solution correspondingly causes 100% and 0% hemolysis.

Cellular uptake and intracellular distribution

For cellular uptake studies, fluorescein-labeled plasmid was produced by conjugating the fluorescein to the luciferase plasmid using *Label* IT® Tracker™ Intracellular Nucleic Acid Localization Kit (Mirus, Madison, WI) according to the manufacturer's protocol. HepG2 cells were seeded in a 24-well plate at the density of 5×10^4 cells/well and were incubated in DMEM medium with 10% FBS at 37 ºC overnight. Polyplex samples containing 1 μg of the fluorescein-labeled plasmid were added to the cells and the HepG2 cells were incubated at 37 ºC for additional 6 h. After the incubation, the culture media were removed and the cells were rinsed with PBS solution (0.01 M, pH = 7.4) three times. Subsequently, the treated cells were harvested using trypsin and centrifuged at 1,500 rpm for 5 min. Upon removal of supernatants, the cells in each well were resuspended in 0.5 mL of cold PBS and were analyzed to measure fluorescein contents using FACSCallibur (Becton Dickinson, San Jose) at excitation wavelength of 488 nm. Data collection involved 10,000 counts per sample.

Confocal Laser Scanning Microscopy (CLSM) was used to visualize the internalization of polyplex particles containing fluorescein-labeled plasmid by HepG2 cells. Cells were seeded on 15 mm glass slides at the density of 5×10^4 cells/slide and were incubated in DMEM medium with 10% FBS at 37 ºC overnight. Different polyplex formulations containing 1 μg fluorescein-labeled plasmid were added to each slide and the cells were incubated at 37 ºC for additional 6 h or 24 h. Subsequently, the culture media were removed and the cells were washed twice with cold PBS. After staining the cell nuclei with Hoechst 33342 (10 μg/mL), the intracellular distribution of fluorescein-labeled plasmid was observed by CLSM using a Lecia TCS SP5 Spectral Confocal Microscope. The excitation wavelength for detecting Hoechst 33342 and fluorescein was 405 nm and 492 nm, respectively.

In vitro cytotoxicity of TRAIL gene-loaded mTAT-quaternary polyplex

The *in vitro* therapeutic efficacy of DNA/NLS/PPMS/PGA-*g*-PEG-mTAT quaternary polyplex bearing TNF-related apoptosis-inducing ligand (TRAIL) gene was measured against HepG2 cells using MTT assay. The cells were seeded in a 96-well plate at a density of 1×10^4 cells/well in DMEM medium (100 μL/well) with 10% FBS at 37 °C in 5% CO_2 atmosphere. After the cells were allowed to adhere overnight, the medium was removed and the mTAT-quaternary polyplex encapsulating 0.5 μg of EGFP or TRAIL gene in 100 μL of the DMEM/FBS medium was added to each well. LF2K was used instead of PPMS as the positive control. After 48 h incubation, the cell viability was quantified by MTT assay.

Western blot analysis

The gene expression efficiency of TRAIL gene in the mTAT-quaternary polyplex (DNA/NLS/PPMS/PGA-PEG-mTAT) and binary polyplexes were determined at protein level by western blot analysis. The intensity of bands on a western blot was quantified using Adobe Photoshop CS4 software. In addition, naked TRAIL gene and LF2K/TRAIL lipoplexes were used as the negative control and positive control, respectively. In typical procedures, HepG2 cells were seeded in a 24-well plate at a density of 7.5×10^4 cells/well and the polyplex samples containing 1μg of TRAIL gene were added to each well. After 48 h incubation, total protein was extracted from the cells and the protein concentration was quantified using BCA protein assay kit. For western blot assay, 20 μg of protein samples were loaded, separated by 12% SDS-PAGE, and then transferred onto polyvinylidene difluoride (PVDF) membranes at 300 mA for 45 min. The PVDF membranes were subsequently incubated in a blocking buffer containing 5% low fat milk, 150 mM NaCl and 20 mM Tris-HCl (pH = 7.5) at 4 ºC overnight. The blocked membranes were incubated with a mouse antibody against the TRAIL (1:500 dilution) and β-actin (1:4000 dilution). Thereafter, the membranes were probed with a secondary antibody, horseradish peroxidase (HRP)-conjugated anti-mouse IgG (1:5000 dilution), in 5% low fat milk at room temperature for 2 h. The blots were developed by using an ECL kit. Finally, the membranes were exposed by using gel imaging and analysis system (ProteinSimple, FluorChem Q).

***In vivo* gene transfection study**

For *in vivo* luciferase expression evaluation, 7-8 weeks old female BALB/C mice weighting 18-22 g were purchased and maintained in the Center for Experimental Animals (an AAALAC accredited experimental animal facility) at Sun Yat-sen University. To establish tumors, mice were injected with 2×10^6 CT-26 tumor cells (GGT positive murine cell line) subcutaneously. When the tumors reached 100~200 mm^3 in size, the mice were divided into four groups (five mice per group) for *in vivo* gene transfection studies. Different formulations (200 μL) were administered to the mice at a dose of 20 μg DNA per mouse via tail-vein injection as follows: group A treated with LucDNA/PPMS binary polyplex, group B with LucDNA/NLS/PPMS/PGA-*g*-PEG-mTAT quaternary polyplex, group C with naked LucDNA, and group D with LucDNA/Lipofectamine™ 2000 lipoplex. After 48 h, the mice were euthanized and their organs including heart, liver, spleen, lung, kidney and tumor were collected. The organs were rinsed twice with normal saline, weighed and homogenized in 25% (w/v) lysis buffer (Promega) using an IKA T25 digital ultra-turrax homogenizer (Germany). After freezing and thawing, the homogenate samples were centrifuged at 12,000 rpm for 10 min and the supernatants (20 μL) were mixed with luciferase substrate reagent (100 μL) to measure luciferase activity. The luciferase activity was reported as values in RLU/mg of tissue.

Statistical analysis

All data are reported as the means ± standard deviations from at least three repeated experiments. Statistical analyses were performed using a two-sided Student's T-test. A *P*-value of 0.05 or less is considered to be statistically significant.

Results and discussion

PPMS copolymer preparation

Poly(*ω*-pentadecalactone-*co*-*N*-methyldiethyleneamine-*co*-sebacate) (PPMS) copolymers were synthesized via copolymerization of *ω*-pentadecalactone (PDL) with diethyl sebacate (DES) and *N*-methyldiethanolamine (MDEA) in diphenyl ether using *Candida antarctica* Lipase B (CALB) as a catalyst according to the method described in our previous report.[12] The PPMS copolymer employed in this work contained 10 mol% PDL units vs. (PDL + sebacate) units and had a M_w of 20400 Da and M_w/M_n of 1.9. NMR spectroscopy analysis showed that the copolymer possessed random distribution of the repeat units along the polymer chains.

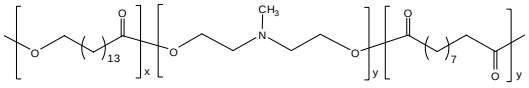

PPMS Structure

Optimization of γ-PGA coating

Nanoparticles with excessive positive surface charges are not stable in physiological fluids and have a short circulation time in the blood *in vivo*. To enhance the *in vivo* efficacy of cationic polyplex particles, it is necessary to reduce or neutralize the positive charges of the particles. Thus, the LucDNA/PPMS binary polyplex particles were surface-modified with γ-PGA, a naturally occurring anionic poly(amino acid). Normally, negatively charged polyplexes have a low cellular uptake rate since they are electrostatically repelled by the negatively charged cell membranes.[19] Nevertheless, because γ-PGA can be recognized by and attracted to certain cells containing an intrinsic membrane protein, γ-glutamyl transpeptidase (GGT), anionic nanoparticles with γ-PGA bound on the surface can efficiently cross the plasma membrane via a specific GGT-mediated pathway and often exhibit expedite cellular internalization by GGT-positive cell lines.[19, 28]

Table 1. The size, PDI and zeta potential of ternary PPMS/LucDNA/γ-PGA polyplexes. Data are given as mean ± SD (n = 3).

N/C ratio [a]	Size (nm)	PDI	Zeta Potential (mV)
1	222 ± 56	0.140	-42.1 ± 0.1
5	828 ± 112	0.532	-15.5 ± 3.3
30	852 ± 362	0.556	+3.7 ± 4.2
50	784 ± 248	0.485	+3.1 ± 2.8
70	369 ± 115	0.543	+5.2 ± 1.5
100	241 ± 27	0.386	+7.5 ± 1.5
0 [b]	164 ± 29	0.383	+68.2 ± 13.2

a. Molar ratio of the amino groups in PPMS to the carboxyl groups in γ-PGA.
b. Binary PPMS/LucDNA polyplex at N/P ratio of 150.

The results of our previous study show that the optimal N/P ratio for LucDNA/PPMS binary polyplex is 150:1. Therefore,

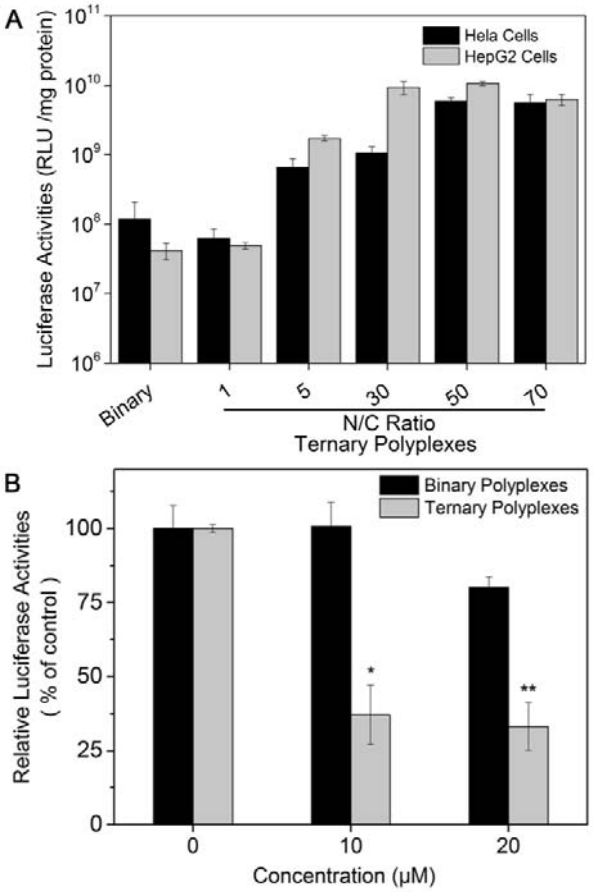

Figure 1. Gene transfection efficiency of the ternary PPMS/LucDNA/γ-PGA polyplex: (A) against Hela cells (GGT negative cells line) and HepG2 cells (GGT positive cells line), (B) against HepG2 cells after the cells were pretreated with free γ-PGA (5 kDa) at different concentrations. The binary PPMS/LucDNA polyplex was used as a reference sample for comparison. Data are given as mean ± SD (n = 3). * represents $p<0.05$, ** represents $p<0.01$.

this N/P ratio was employed to formulate ternary and quaternary polyplexes. To maximize the potency of LucDNA/PPMS/γ-PGA ternary polyplex, the amount of γ-PGA was varied to determine the optimal N/P/C ratio for the polyplex. As shown in Table 1, increasing the amount of γ-PGA gradually decreases the zeta potential of the ternary polyplex from +68.2 mV to –42.1 mV. This result indicates that γ-PGA was successfully coated on the surface of LucDNA/PPMS binary polyplex particles. Despite the size increase (from 164 nm to 222-852 nm) of the ternary polyplex particles upon modification with γ-PGA, the ternary system at N/C ratio from 5 to 70 exhibited higher efficiency than the binary polyplex in transfecting both HepG2 cells (GGT positive cell line) and Hela cells (GGT negative cell line) (Figure 1A). In particular, at N/C ratio of 50:1, the transfection efficiency of the ternary polyplex in HepG2 cells and Hela cells was respectively 255-fold and 50-fold as high as that of the binary polyplex. It is notable that LucDNA/PPMS binary polyplex is

less efficient in transfecting HepG2 cells vs. Hela cells, whereas higher efficiency was observed for LucDNA/PPMS/γ-PGA ternary polyplex in transfecting HepG2 cells at N/C ratio of 5-70 (Figure 1A). This result indicates that the surface modification with γ-PGA enhances the interactions between the ternary polyplex and GGT positive HepG2 cells more significantly compared with the interactions between the polyplex and GGT negative Hela cells. Additionally, when HepG2 cells were pre-treated with free γ-PGA at different concentrations (10-20 μM) and subsequently incubated with polyplex particles, the luciferase expression in the cells remained nearly constant or slightly lower for the binary polyplex but decreased dramatically for the ternary polyplex sample (Figure 1B) due to the blockage of GGT-mediated pathway. Similar phenomena were previously observed for Chitosan/DNA/γ-PGA polyplexes[18,19] and PEI/DNA/γ-PGA polyplexes,[20] showing that the γ-PGA coating on the binary polycation/DNA polyplexes significantly enhanced their gene transfection efficacy due to increased cellular uptake efficiency via a specific GGT-mediated endocytic pathway.

Optimization of DNA/NLS/PPMS/PGA-*g*-PEG-mTAT (mTAT-quaternary polyplex) formulation

As the results in section "Optimization of γ-PGA coating" show, γ-PGA coating of DNA/PPMS polyplex enhances the transfection efficiency of the polyplex particles. However, the surface modification with γ-PGA significantly increases the average size of the resultant DNA/PPMS/γ-PGA ternary polyplex (Table 1). To achieve desirable passive targeted delivery of nanoparticles to solid tumors via enhanced permeation and retention (EPR) effect, it is important to control the size of the particles below 400 nm in diameter.[29, 30] We discovered that by grafting 5-20% PEG to γ-PGA and using the resultant PGA-*g*-mPEG to coat PPMS/DNA binary polyplex particles, PPMS/DNA/γ-PGA-*g*-mPEG particles were formed in smaller sizes. For example, at the N/C ratio of 100, the average size of PPMS/DNA/γ-PGA-*g*-mPEG polyplexes with 5%, 10% and 20% PEG was 228 nm, 191 nm and 166 nm, respectively, which are smaller than the average size of DNA/PPMS/γ-PGA ternary polyplex (241 nm). Upon changing the N/C ratio from 100 to 5, the average size of PPMS/DNA/γ-PGA-*g*-mPEG polyplex with 10% PEG further decreased from 191 nm to 126 nm.

The incorporation of hydrophilic PEG shell in PPMS/DNA/PGA-*g*-mPEG polyplex appears to substantially enhance the stability of the polyplex particles in aqueous medium. As shown in Fig. 2A, upon incubation in PBS (0.01 M, pH = 7.4) containing 10% (v/v) fetal bovine serum (FBS) at 37 °C for 24 h, the average size of the ternary polyplexes modified with PGA-*g*-mPEG remained nearly constant during the whole incubation period. In contrast, the average size of the ternary PPMS/DNA/γ-PGA polyplex with 0% PEG increased rapidly from 242 nm to 1157 nm within the same period of time. The improved stability of the PPMS/DNA/PGA-*g*-mPEG polyplex is crucial to prolong circulation of the polyplex particles *in vivo* and to effectively achieve passive targeted gene delivery to tumors.

Fig. 2B shows the luciferase gene transfection efficiency of various ternary PPMS/DNA/PGA-*g*-mPEG polyplexes at different N/C ratios against HepG2 cells. At a low N/C ratio (e.g., N/C = 5), the luciferase protein expression of the ternary polyplexes decreased significantly with increasing percentage of the PEG grafting presumably due to reduced cellular uptake rates of the polyplex particles caused by the PEGylation.[31-33] However, this detrimental effect diminishes at higher N/C ratios and at N/C ratio = 100, the luciferase expression of the ternary polyplex with 10% PEG is approximately 8.5-fold as high as that of the binary PPMS/LucDNA polyplex and 1.2-fold as high as that of the ternary polyplex with 0% PEG. On the basis of these results, the ternary PPMS/DNA/PGA-*g*-mPEG polyplex with 10% PEG and the N/C ratio of 100 were selected for the subsequent studies.

We hypothesize that the nuclear uptake of DNA could be improved by incorporating the NLS peptide into the ternary polyplex to form quaternary PPMS/DNA/NLS/PGA-*g*-mPEG polyplex. Since transportation of DNA into the nucleus is a key step in gene transfection processes, accelerated nuclear uptake of DNA is expected to increase the transfection efficiency of the quaternary polyplex. Thus, the gene transfection efficiency of PPMS/LucDNA/NLS/PGA-*g*-mPEG polyplex was evaluated at various NLS/DNA ratios ranging from 5 to 20 (NLS/DNA ratio is defined as the molar ratio of nitrogen residues of NLS to phosphate residues of DNA). The results showed that the transfection efficiency of the quaternary polyplexes were significantly higher than that of either the binary PPMS/LucDNA polyplex or the ternary PPMS/LucDNA/PGA-*g*-mPEG polyplex with the highest transgene expression level observed at NLS/DNA ratio of 10:1 (Figure 2C). At 10:1 ratio of NLS/DNA, the quaternary polyplex was 337-fold more potent than the binary polyplex and 19-fold more potent than the ternary polyplex. These results confirm our earlier hypothesis that the transfection efficiency of PPMS-based non-viral gene vectors could be enhanced by additionally incorporating an NLS peptide into the carriers.

As discussed above, PEGylation to construct a PEG shell in the polyplex particles is essential to stabilize the particles in aqueous medium. However, the PEGylation also inhibits the particle interactions with cells and reduces cellular uptake rate. To recover and further improve the uptake rate of PPMS/DNA/NLS/PGA-*g*-PEG polyplex by cells, mTAT peptide was covalently linked to PGA-*g*-PEG to form PGA-*g*-PEG-mTAT conjugate (the grafting percentage of mTAT was 94%) and PPMS/LucDNA/NLS/PGA-*g*-PEG-mTAT polyplexes (or mTAT-quaternary polyplexes) were prepared by replacing a portion (20-80 mol%) of PGA-*g*-mPEG with PGA-*g*-PEG-mTAT in PPMS/LucDNA/NLS/PGA-*g*-mPEG particles. The results on gene transfection in HepG2 cells showed enhanced efficacy of the mTAT-quaternary polyplexes, which is dependent on mTAT content in the polyplex samples (Figure 2D). At the optimal mTAT content (i.e., 40 mol%), the gene expression level was 1.4-fold as that of the unmodified

PPMS/LucDNA/NLS/PGA-*g*-mPEG polyplex and approximately 3.3-fold as that of commercial LF2K/LucDNA lipoplex (Figure 2D). Thus, incorporation of mTAT is effective to overcome the 'PEG dilemma' phenomenon and to improve the cellular uptake of the quaternary polyplexes. More details regarding the cellular uptake rate are discussed in the latter section "Cellular uptake".

Consistent with the above results on luciferase gene transfection, transfection experiments using pEGFP plasmid-loaded polyplex formulations also demonstrated that incorporation of NLS and mTAT functional peptides significantly improves gene transfection capability of the quaternary PPMS/DNA/NLS/PGA-*g*-PEG-mTAT system. As shown in Fig. 2E, modification of PPMS/pEGFP binary polyplex with PGA-*g*-mPEG yielded the ternary PPMS/pEGFP/PGA-*g*-mPEG polyplex with substantially higher efficiency in GFP expression. The gene transfection

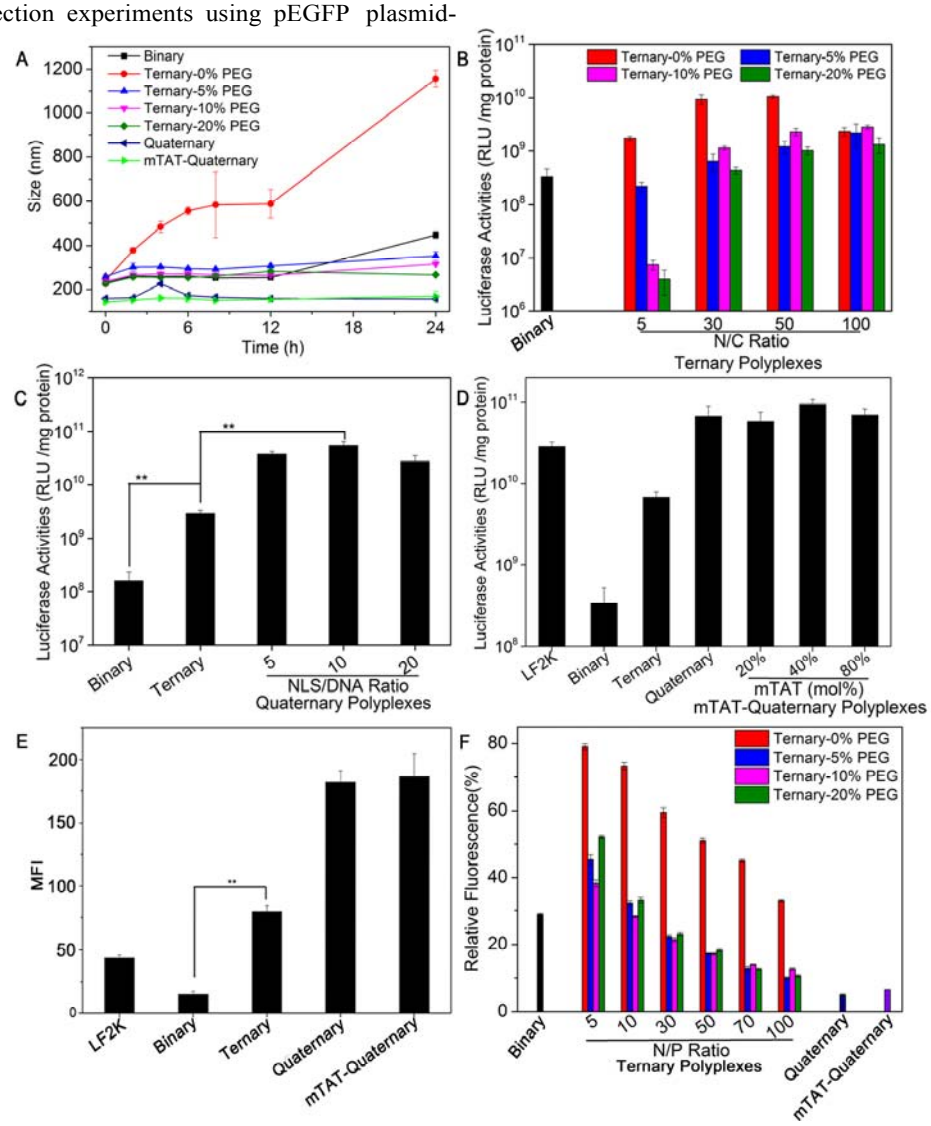

Figure 2. Stability and gene transfection efficiency of the ternary PPMS/LucDNA/PGA-*g*-PEG, quaternary PPMS/LucDNA/NLS/PGA-*g*-PEG and mTAT-quaternary PPMS/LucDNA/NLS/PGA-*g*-PEG-mTAT polyplex nanoparticles: (A) average particle size vs. incubation time for the polyplexes with N/C ratio of 100 incubated in PBS (0.01 M, pH = 7.4) containing 10% FBS; (B) transfection efficiency of the ternary PPMS/LucDNA/PGA-*g*-PEG polyplexes with 0-20% PEG grafting at various N/C ratios against HepG2 cells; (C) transfection efficiency of the quaternary PPMS/LucDNA/NLS/PGA-*g*-PEG polyplexes with various NLS/DNA ratios against HepG2 cells (the data on the binary polyplex and the ternary polyplex with N/C ratio of 100 are included for comparison); (D) transfection efficiency of the mTAT-quaternary polyplexes with various mTAT contents against HepG2 cells; the results on the binary polyplex, the ternary polyplex with N/C ratio of 100, the quaternary polyplex with NLS/DNA ratio of 10 and the LF2K/DNA lipoplex are included for comparison; (E) mean fluorescence intensities of the HepG2 cells after being transfected with the optimal binary, ternary, quaternary and mTAT-quaternary polyplexes carrying pEGFP and with LF2K/pEGFP lipoplex; (F) results of Gel Red exclusion assay on the binary, ternary (with various PEG contents and N/C ratios), quaternary and mTAT-quaternary polyplexes. Where it was necessary, the binary PPMS/DNA polyplex was also used as a reference sample for comparison. Data are given as mean ± SD (n = 3). ** represents $p<0.01$.

Table 2. Characterization of the optimized binary, ternary, quaternary and mTAT-quaternary polyplex particles. Data are given as mean ± SD (n = 3).

Sample [a]	Size (nm)	PDI	Zeta Potential (mV)
Binary polyplex	164 ± 29	0.383	68.2 ± 13.2
Ternary polyplex	191 ± 18	0.186	8.0 ± 1.3
Quaternary polyplex	221 ± 13	0.317	9.3 ± 2.9
mTAT-Quaternary polyplex	179 ± 22	0.345	12.6 ± 1.2

a: The binary, ternary, quaternary and mTAT-quaternary polyplexes represent PPMS/LucDNA, PPMS/LucDNA/PGA-*g*-mPEG, PPMS/LucDNA/NLS/PGA-*g*-mPEG, and PPMS/LucDNA/NLS/PGA-*g*-PEG-mTAT, respectively.

efficiency was further increased upon incorporation of NLS into the ternary polyplex to form the quaternary PPMS/pEGFP/NLS/PGA-*g*-mPEG system and the highest mean fluorescence intensity of GFP was exhibited by the mTAT-quaternary polyplex, which is approximately 4.3-fold as that of LF2K/pEGFP lipoplex. These results are in line with the literature reports on enhanced gene transfection efficiency by additionally incorporating nuclear localization signals and cell-penetrating peptides into polyplex gene vectors.[5, 34, 35]

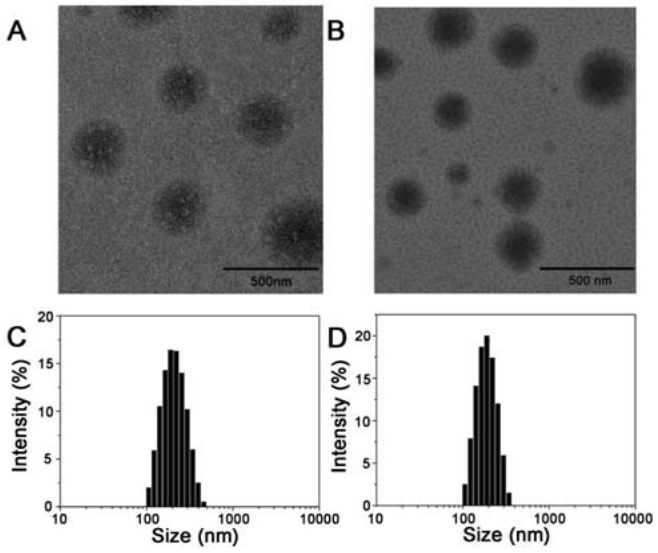

Figure 3. The TEM images and particle size distributions of the ternary PPMS/LucDNA/PGA-*g*-PEG polyplex (A, C) and mTAT-quaternary polyplex (B, D).

The physicochemical properties and morphology of these optimized polyplexes are shown in Table 2 and Figure 3. The mean size of the polyplex particle samples is in a desirable range between 164 nm and 221 nm. Due to the incorporation of PGA-*g*-mPEG, the ternary polyplex had a dramatically decreased zeta potential of 8.0 mV compared with the zeta potential of 68.2 mV for the binary system (Table 2). Similarly, the zeta potential values of the quaternary polyplex and mTAT-quaternary polyplex were 9.3 mV and 12.6 mV, respectively. TEM images showed that the ternary polyplex particles and the mTAT-quaternary polyplex particles were nearly spherical in shape and possessed a narrow particle size distribution (Fig. 3A and 3B). The sizes of both polyplex samples were confirmed by DLS analysis (Fig. 3C and 3D). In addition, the quaternary polyplex and mTAT-quaternary polyplex remained stable during the whole incubation period (Fig. 2A), indicating that the modification with the NLS and mTAT peptides has minimal effects on the stability of the polyplexes

Dye exclusion assay

Strong DNA-binding capability of cationic polymers is crucial for formulating polyplexes with high gene transfection efficiency. To determine how the incorporation of PGA-*g*-mPEG, PGA-*g*-PEG-mTAT and NLS affects the DNA condensation ability of the ternary and quaternary polyplexes, dye exclusion assay experiments were performed. During the experimental procedures, the gel red was incubated with free DNA or DNA-loaded polyplex particles. The fluorescence of the dye molecules significantly increases when they intercalate between the bases of DNA. High fluorescence is typically produced with free plasmid DNA, but the fluorescence signal becomes much weaker when DNA is bound to cationic polymer chains that prevent effective dye-DNA interactions.[36]

As depicted in Figure 2F, upon treatment with the gel red dye, the ternary polyplexes with 0% PEG at N/C ratio between 5 and 100 exhibited higher fluorescence intensity than the binary PPMS/DNA polyplex. This result indicates that DNA is less strongly bound in the ternary system with 0% PEG compared with the binary system, which could be attributed to the disruption of electrostatic interactions between PPMS and DNA by the anionic γ-PGA in the ternary polyplexes. Upon conjugation of 5-20 mol% PEG to the γ-PGA, the resultant PPMS/DNA/PGA-*g*-mPEG polyplexes possessed enhanced DNA-binding ability that is dependent on N/C ratio of the polyplexes with the higher N/C ratio promoting the DNA condensation (Figure 2F). Thus, at the N/C ratio of 100, the relative fluorescence intensity values for the ternary polyplex samples with 5% PEG, 10% PEG and 20% PEG were respectively 9.9%, 12.6% and 10.5%. These values are substantially lower than the relative fluorescence intensity of the binary polyplex (28.8%) possibly due to the shielding effects of the PEG shells. Furthermore, because of the cationic sequence structures present in the NLS and mTAT, the

DNA condensation capability was even stronger for the quaternary polyplex and the mTAT-quaternary polyplex whose relative fluorescence intensity values were 5.0% and 6.6%, correspondingly (Figure 2F).

In vitro cytotoxicity and hemolysis assay

Cytotoxicity of the ternary polyplex, quaternary polyplex and mTAT-quaternary polyplex was evaluated on HepG2 cells by MTT assay. As shown in Fig. 4A, all three polyplex samples did not show obvious cytotoxicity as the viability of the cells treated with each of these polyplexes remained over 80% even at the highest polyplex concentration of 600 μg/mL. For comparison, the viability of the cells treated with the binary PPMS/LucDNA polyplex was similar at ≤ 400 μg/mL concentration, but significantly lower (~62%) at the high concentration of 600 μg/mL. The above polyplex samples were also incubated with erythrocytes to evaluate their blood compatibility and the results are shown in Fig. 4B. At polyplex concentration of 250 μg/mL, erythrocyte agglutination was observed for the binary polyplex, but not detected for the ternary, quaternary and mTAT-quaternary systems. Quantitative hemolysis analysis revealed that all polyplex samples had low hemolysis activity (< 8%) at concentration ≤ 250 μg/mL (Fig. 4C). However, at 500 μg/mL concentration, the hemolysis activity of the binary polyplex was much higher (34% vs < 10%) than that of the other three multi-component polyplexes modified with PGA-*g*-PEG. Thus, incorporation of PGA-*g*-PEG or PGA-*g*-PEG-mTAT provides an efficient method to reduce cytotoxicity and hemolysis activity of the multifunctional polyplex particles, which is attributable to their decreased positive surface charge due to PGA-*g*-PEG shielding.

Cellular uptake

Cellular uptake is one of several important steps that influence gene delivery and transfection efficiency of polyplexes. To understand how the modifications with PGA-*g*-PEG, NLS and mTAT affect the cellular uptake of polyplexes, the binary PPMS/DNA, ternary PPMS/DNA/PGA-*g*-PEG, quaternary PPMS/DNA/NLS/PGA-*g*-PEG, and mTAT-quaternary PPMS/DNA/NLS/PGA-*g*-PEG-mTAT polyplexes carrying fluorescein-labeled LucDNA were incubated with HepG2 cells and the intracellular fluorescence intensity of the cells were measured by flow cytometry. Figure 5 shows the mean fluorescence intensity (MFI) (Figure 5A) and fluorescent histogram (Figure 5B) of the HepG2 cells after incubation for 6 h. Among the polyplex samples, the MFI of the cells follows the order: the binary polyplex < the ternary polyplex < quaternary polyplex < mTAT-quaternary polyplex.

Usually, polyplex particles with higher positive surface charges tend to have stronger electrostatic interactions with negatively-charged cell membranes, facilitating cellular uptake to enhance gene transfection. However, despite its lower positive surface charge, the ternary PPMS/DNA/PGA-*g*-PEG polyplex exhibited higher cellular uptake rate than the binary PPMS/DNA polyplex (Figure 5A). This PGA-*g*-PEG-promoted cellular uptake of the ternary polyplex is likely due to the polyplex internalization via a γ-PGA-specific, receptor-mediated endocytosis process, which was inhibited by

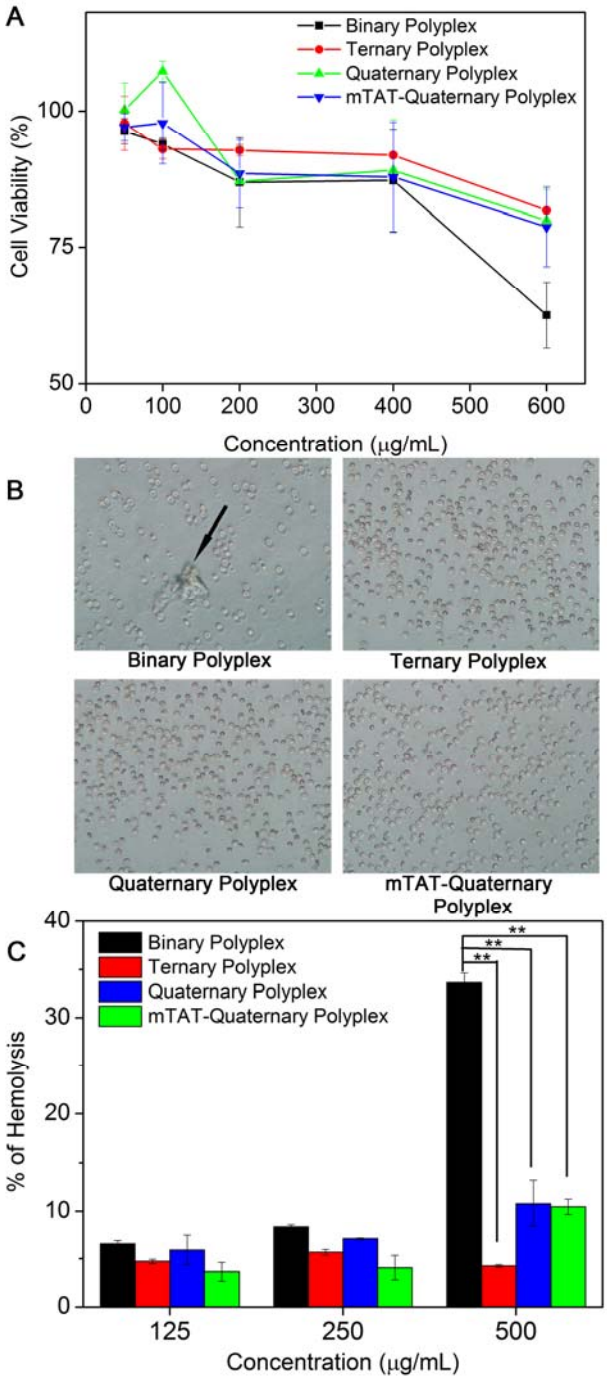

Figure 4. Cytotoxicity of the binary, ternary, quaternary and mTAT-quaternary polyplexes carrying LucDNA: (A) viability of the HepG2 cells after treatment with the polyplex samples at different concentrations, (B) microscopic images (400× magnification) of the erythrocytes after treatment with the polyplexes at 250 μg/mL concentration, and (C) quantitative analysis on hemolysis activity of the polyplexes at different

sample concentrations. Data are given as mean ± SD (n = 3). ** represents $p<0.01$.

pretreatment of the cells with γ-PGA as discussed earlier. NLS also enhances the cellular uptake as the quaternary polyplex was internalized by the cells significantly faster than the ternary system. The observed result could be attributed to the presence of cationic amino groups in NLS, which is capable of electrostatically binding to various anionic species on the extracellular surface to facilitate the cellular uptake of the NLS-

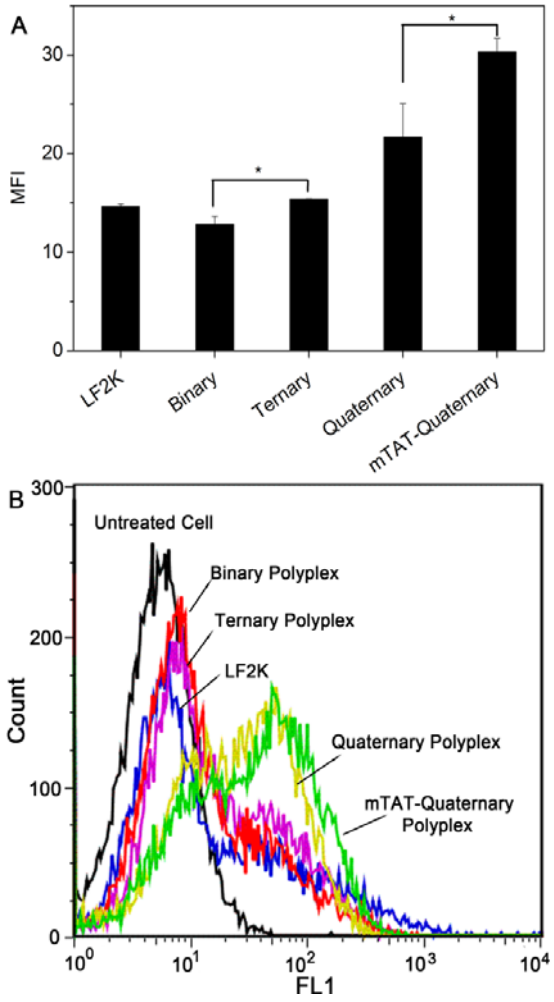

Figure 5. Mean fluorescence intensities (A) and fluorescence histograms (B) of the HepG2 cells incubated for 6 h with the binary, ternary, quaternary, and mTAT-quaternary polyplexes bearing fluorescein-labeled LucDNA. The lipoplex of LF2K and the plasmid was used as a reference. Data are given as mean ± SD (n = 3). * represents $p<0.05$.

modified particles.[37-39] Because of the intense electrostatic interactions and hydrogen bonding between CPPs peptides and moieties on the cell surface, incorporation of mTAT can substantially enhance the binding of the mTAT-quaternary polyplex to the cells and allows further increase in cellular uptake rate of the multi-functional polyplex particles.[40] Thus, the MFI value of the HepG2 cells treated with mTAT-quaternary system was approximately 1.4-fold as that of the quaternary polyplex and 2-fold as that of the ternary polyplex.

Intracellular distribution of NPs

Confocal laser scanning microscopy (CLSM) was used to visualize the cellular uptake of the polyplex particles and to examine the plasmid DNA transport to the nucleus after HepG2 cells were incubated with the binary, ternary, quaternary, and mTAT-quaternary polyplex samples carrying fluorescein-labeled LucDNA for 6 and 24 h. As shown in Fig. 6A, at 6 h, only very weak green fluorescence signal was observed in the cells treated with the binary polyplex due to limited cellular uptake of the polyplex particles. The fluorescence signal was stronger in the cell groups treated with the ternary and quaternary polyplex samples, and the cells incubated with mTAT-quaternary polyplex displayed strongest green fluorescence intensity. At 24 h of incubation time, the green fluorescence signals for all cell groups studied intensified (Fig. 6B). It is important to note that for the cell groups treated with the quaternary and mTAT-quaternary polyplexes, a large portion of the green fluorescence appeared in the nucleus and perinuclear regions, whereas most of the fluorescein-labeled DNA in the binary and ternary polyplex samples existed in the cytoplasma. Thus, incorporation of NLS peptide is effective in promoting intracellular delivery of the plasmid to the nuclei. Nuclear transport of DNA is known to be the rate-limiting step in gene transfection process as the nuclear envelope represents the most substantial barrier in gene delivery.[41, 42] As shown in an earlier section, inclusion of NLS functional peptide is crucial to yield high gene transfection efficiency of the mTAT-quaternary polyplex.

***In vitro* therapeutic efficacy of TRAIL gene-loaded mTAT-quaternary polyplex**

The ability of the multi-functional PPMS/TRAIL/NLS/PGA-*g*-PEG-mTAT polyplex to inhibit growth of tumor cells was evaluated in this study. It is known that the therapeutic TRAIL gene is capable of killing a variety of human tumor cells and inhibiting tumor-related angiogenesis, but is not harmful to normal cells.[43,44] The TRAIL gene was expressed in HepG2 tumor cells and the protein level in the cells after the gene expression was examined by western blotting assay. As shown in Fig. 7A and 7B, the gene transfection with the TRAIL-loaded mTAT-quaternary polyplex resulted in 1.5-fold TRAIL protein expression vs. that obtained with the binary PPMS/TRAIL polyplex. The *in vitro* cytotoxicity induced by loaded mTAT-quaternary polyplex was determined by MTT assay, and pEGFP-loaded mTAT-quaternary polyplex was used as a negative control. As depicted in Fig. 7C, the viability of the cell groups treated with pEGFP-loaded mTAT-quaternary polyplex and TRAIL-loaded mTAT-quaternary polyplex was 81% and 62%, respectively. Thus, the cell viability results are consistent with the data of western blotting assay. The overall experimental results reveal that the blank vector has low

cytotoxicity and the efficacy of TRAIL-loaded mTAT-quaternary system in killing HepG2 tumor cells is primarily attributable to the TRAIL protein expression in the cells as the result of successful transfection of therapeutic TRAIL gene.

In vivo gene transfection

Murine CT-26 cells were used to establish subcutaneous tumors in BALB/C mice due to their high expression of GGT.[45] To ensure that the gene transfection efficiency of the mTAT-quaternary polyplex is comparable against CT-26 cells vs. HepG2 cells, *in vitro* LucDNA transfection was performed in CT-26 cells. The results showed that there was essentially no difference in LucDNA expression level between the two cell lines (data not shown). The gene expression in different types of tissues and tumors of the mice were analyzed 48 h after single tail vein injections of the binary PPMS/LucDNA

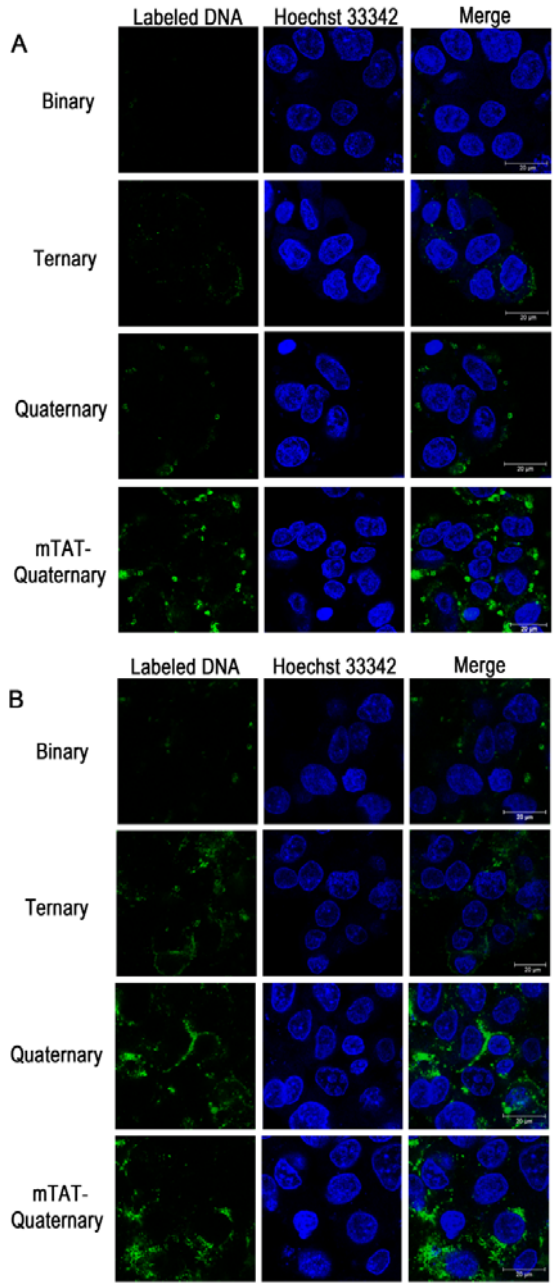

Figure 6. Confocal Laser Scanning Microscope (CLSM) images of the HepG2 cells incubated with the binary, ternary, quaternary, and mTAT-quaternary polyplexes carrying fluorescein-labeled LucDNA for 6 h (A) and 24 h (B).

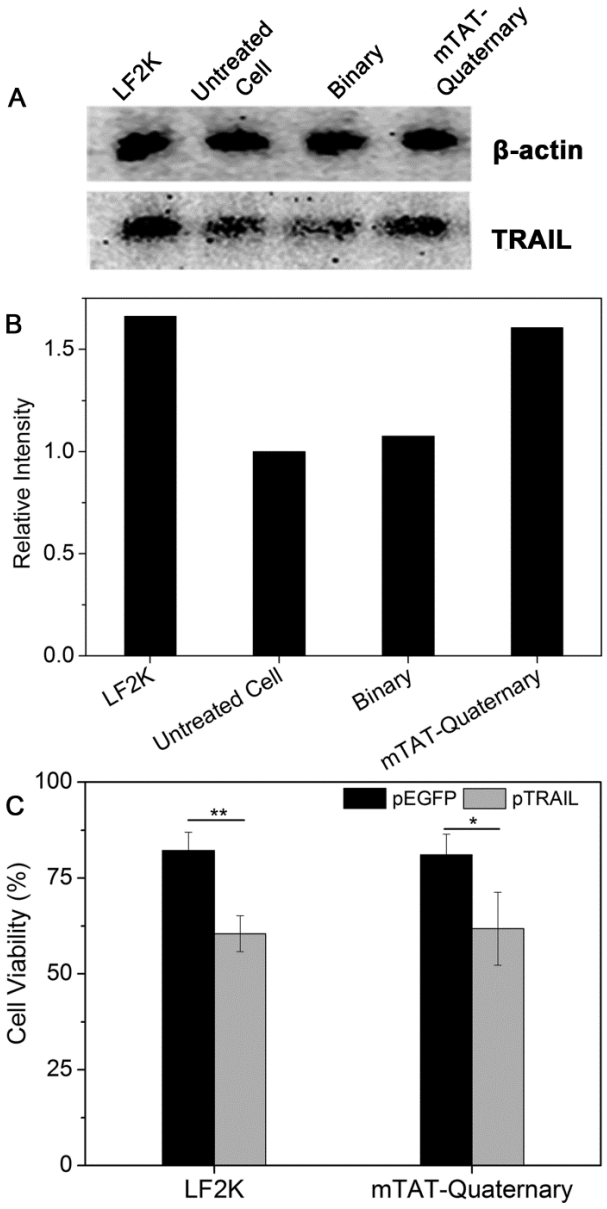

Figure 7. Efficiency of the binary and mTAT-quaternary polyplexes bearing TRAIL in transfecting HepG2 cells: (A) TRAIL expression levels in the cells, (B) quantitative analysis of the Western blot bands using Photoshop software with β-actin as control, and (C) viability of the HepG2 cells incubated for 48 h with TRAIL or EGFP-loaded LF2K lipoplexes and mTAT-quaternary polyplexes. Data are given as mean ± SD (n = 3). * represents $p<0.05$, ** represents $p<0.01$.

polyplex, quaternary PPMS/LucDNA/NLS/PGA-*g*-PEG-mTAT polyplex, naked LucDNA, and LF2K/LucDNA lipoplex. The obtained *in vivo* gene transfection results are shown in Figure 8. In general, low LucDNA transfection was observed in the heart, liver, spleen and kidney for all formulations and enhanced LucDNA transfection was observed in the tumor for three nanoparticle samples (the binary polyplex, mTAT-quaternary polyplex and LF2K/LucDNA lipoplex) but not naked LucDNA. This is likely due to the EPR effect which allows the delivery of the particle samples passively targeting at the tumor sites. Among the three particle samples, the mTAT-quaternary polyplex exhibited the highest gene transfection

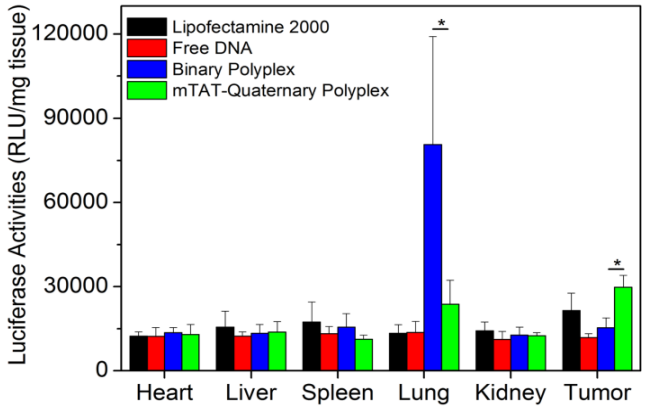

Figure 8. Luciferase gene expression efficiencies in the major organs and tumors of Balb/c mice at 48 h after intravenous injection of the naked LucDNA, LucDNA/LF2K lipoplex, the binary PPMS/LucDNA and PPMS/LucDNA/NLS/PGA-g-PEG-mTAT (mTAT-quaternary) polyplexes. The mice were sacrificed 2 days after injection and their organs and tumors were dissected to quantify luciferase expression. *represents $p<0.05$ compared with the binary polyplex. Each bar represents the mean ± SD (n= 5).

level in the tumor with the gene expression signal which is significantly higher than that generated by LF2K/LucDNA lipoplex and is approximately twice as strong as that generated by the binary polyplex. The lipoplex particles are known to possess high cytotoxicity and are unstable under *in vivo* physiological conditions although they are quite efficient vectors for *in vitro* delivery of DNA to cells. The binary PPMS/LucDNA polyplex particles contain substantial positive charges on the surface (Table 1) and tend to aggregate in serum-containing aqueous medium (Figure 2A), which render them vulnerable to elimination from the blood by reticuloendothelial system. Our results suggest that the remarkable efficiency of the mTAT-quaternary polyplex particles to transfect the CT-26 tumor cells in mice is attributable to their high stability in serum-containing aqueous medium due to PEG modification (Figure 2A), their enhanced cellular uptake rate due to incorporation of γ-PGA and mTAT functional components (Figure 5), and increased nuclear transportation of DNA due to the inclusion of NLS peptide. Finally, it is interesting to note that the binary PPMS/LucDNA polyplex was substantially active in transfecting the lung cells while the other three samples had low activity toward the organ (Figure 8). This could result from the positive surface charge-promoted aggregation of the polyplex particles with serum proteins, erythrocytes and other blood components to form large agglomerates that can accumulate in vascular beds of the lung.[24, 25, 27]

Conclusions

We have designed and fabricated a multifunctional, non-viral gene delivery platform that consist of cationic poly(amine-*co*-ester) for DNA condensation, PEG shell for nanoparticle stabilization, γ-PGA and mTAT for accelerated cellular uptake, and NLS peptide for enhanced intracellular transport of DNA to the nucleus. In vitro study showed that PGA-*g*-PEG coating led to the formation of the ternary PPMS/DNA/PGA-*g*-PEG polyplex with decreased positive charges, substantially higher stability in serum-containing aqueous medium and enhanced cellular uptake via GGT-mediated endocytosis pathway. The cellular uptake rate and intracellular DNA delivery was further improved by incorporating mTAT and NLS peptides into the ternary polyplex system. As the result, the new quaternary PPMS/LucDNA/NLS/PGA-*g*-PEG-mTAT system exhibited reduced cytotoxicity including hemolysis activity, higher DNA binding capability, remarkably faster cellular uptake rate, and enhanced nuclear transport of DNA compared with the binary PPMS/LucDNA polyplex. All these advantageous functionalities and properties contribute to the remarkable *in vitro* and *in vivo* gene transfection efficiency of the mTAT-quaternary polyplex. The results of this work demonstrate that the multifunctional mTAT-quaternary polyplex system with improved efficiency and reduced cytotoxicity represents a new type of promising non-viral vectors for delivery of therapeutic genes to treat tumors

Acknowledgements

This work was supported by National Natural Science Foundation of China (51103183, 81101142), Guangdong Natural Science Foundation (S2011040001777), Doctoral Fund of Ministry of Education of China (20110171120004), the Project of Zhu Jiang Science and Technology New Star (2012J2200053), the Program for Industry, University & Research Institute Collaboration of Guangdong Province (2012B091100452), the Project of Key Laboratory of Sensing Technology and Biomedical Instruments of Guangdong Province (2011A060901013) and the Fundamental Research Funds for the Central Universities.

Notes and references

[a] Department of Biomedical Engineering, School of Engineering, Sun Yat-sen University, Guangzhou, Guangdong 510006, China
[b] Molecular Innovations Center, Yale University, 600 West Campus Drive, West Haven, Connecticut 06516, United States

[c] Department of Medical Oncology, Sun Yat-sen University Cancer Center, State Key Laboratory of Oncology in Southern China, Guangzhou, Guangdong 510060, China.

References

1 I.M. Verma, N. Somia, *Nature*, 1997, **389**, 239.
2 C. Sawyers, *Nature*, 2004, **432**, 294.
3 H. Lv, S. Zhang, B. Wang, S. Cui, J. Yan, *J. Controlled Release*, 2006, **114**, 100.
4 D. Luo, W.M. Saltzman, *Nat Biotechnol*, 2000, **18**, 33.
5 W.J. Yi, J. Yang, C. Li, H.Y. Wang, C.-W. Liu, L. Tao, S.X. Cheng, R.X. Zhuo, X.Z. Zhang, *Bioconjug. Chem.*, 2012, **23**, 125.
6 T. Merdan, J. Kopeček, T. Kissel, *Adv. Drug Del. Rev.*, 2002, **54**, 715.
7 J.J. Green, R. Langer, D.G. Anderson, *Acc. Chem. Res.*, 2008, **41**, 749.
8 T. Park, J. Jeong, S. Kim, *Adv. Drug Del. Rev.*, 2006, **58**, 467.
9 D.M. Lynn, R. Langer, *J. Am. Chem. Soc.*, 2000, **122**, 10761.
10 J. Liu, Z. Jiang, J. Zhou, S. Zhang, W.M. Saltzman, *J. Biomed. Mater. Res. A*, 2011, **96A**, 456.
11 D.M. Lynn, D.G. Anderson, D. Putnam, R. Langer, *J. Am. Chem. Soc.*, 2001, **123**, 8155.
12 J. Zhou, J. Liu, C.J. Cheng, T.R. Patel, C.E. Weller, J.M. Piepmeier, Z. Jiang, W.M. Saltzman, *Nat. Mater.*, 2011, **11**, 82.
13 C.M. Wiethoff, C.R. Middaugh, *J. Pharm. Sci.*, 2003, **92**, 203.
14 T. Ito, C. Yoshihara, K. Hamada, Y. Koyama, *Biomaterials*, 2010, **31**, 2912.
15 Y.C. Chung, W.Y. Hsieh, T.H. Young, *Biomaterials*, 2010, **31**, 4194.
16 T. Kurosaki, T. Kitahara, S. Kawakami, Y. Higuchi, A. Yamaguchi, H. Nakagawa, Y. Kodama, T. Hamamoto, M. Hashida, H. Sasaki, *J. Controlled Release*, 2010, **142**, 404.
17 Y.H. Lin, F.L. Mi, C.T. Chen, W.C. Chang, S.F. Peng, H.F. Liang, H.W. Sung, *Biomacromolecules*, 2007, **8**, 146.
18 S.F. Peng, M.T. Tseng, Y.C. Ho, M.C. Wei, Z.X. Liao, H.W. Sung, *Biomaterials*, 2011, **32**, 239.
19 Z.X. Liao, S.F. Peng, Y.C. Ho, F.L. Mi, B. Maiti, H.W. Sung, *Biomaterials*, 2012, **33**, 3306.
20 T. Kurosaki, T. Kitahara, S. Fumoto, K. Nishida, J. Nakamura, T. Niidome, Y. Kodama, H. Nakagawa, H. To, H. Sasaki, *Biomaterials*, 2009, **30**, 2846.
21 J. Gu, X. Wang, X. Jiang, Y. Chen, L. Chen, X. Fang, X. Sha, *Biomaterials*, 2012, **33**, 644.
22 S.L. Lo, S. Wang, *Biomaterials*, 2008, **29**, 2408.
23 K.H. Bremner, L.W. Seymour, A. Logan, M.L. Read, *Bioconjug. Chem.*, 2004, **15**, 152.
24 Q. Hu, J. Wang, J. Shen, M. Liu, X. Jin, G. Tang, P.K. Chu, *Biomaterials*, 2012, **33**, 1135.
25 S. Guo, Y. Huang, W. Zhang, W. Wang, T. Wei, D. Lin, J. Xing, L. Deng, Q. Du, Z. Liang, X.J. Liang, A. Dong, *Biomaterials*, 2011, **32**, 4283.
26 X.F. Zhang, W.X. Tang, Z. Yang, X.G. Luo, H.Y. Luo, D. Gao, Y. Chen, Q. Jiang, J. Liu, Z.Z. Jiang, *J. Mater. Chem. B,* 2014, **2**, 4034
27 S. Daubeuf, M. Accaoui, I. Pettersen, N. Huseby, A. Visvikis, M. Galteau, *Biochim. Biophys. Acta-General Subjects*, 2001, **1568**, 67.
28 M.W. Lieberman, R. Barrios, B.Z. Carter, G.M. Habib, R. Lebovitz, S. Rajagopalan, A.R. Sepulveda, Z.-Z. Shi, D.-F. Wan, *Am. J. Pathol.*, 1995, **147**, 1175.
29 E. Gullotti, Y. Yeo, *Mol. Pharm.*, 2009, **6**, 1041.
30 A.A. Gabizon, H. Shmeeda, S. Zalipsky, *J. Liposome Res.*, 2006, **16**, 175.
31 W. Zhang, Q. Cheng, S. Guo, D. Lin, P. Huang, J. Liu, T. Wei, L. Deng, Z. Liang, X.J. Liang, A. Dong, *Biomaterials*, 2013, **34**, 6495.
32 S.D. Li, L. Huang, *J. Controlled Release*, 2010, **145**, 178.
33 S. Guo, L. Huang, J. Nanomater., 2011, **2011**, 1.
34 H.W. Zhang, T. Gerson, M.L. Varney, R.K. Singh, S.V. Vinogradov, *Pharmaceutical Research*, 2010, **27**, 2528.
35 N.M. Moore, C.L. Sheppard, S.E. Sakiyama-Elbert, *Acta Biomaterialia*, 2009, **5**, 854
36 G.T. Zugates, D.G. Anderson, S.R. Little, I.E. Lawhorn, R. Langer, *J. Am. Chem. Soc.*, 2006, **128**, 12726.
37 H. Zhang, S.V. Vinogradov, *J. Control Release*, 2010, **143**, 359.
38 F. Wang, Y. Wang, X. Zhang, W. Zhang, S. Guo, F. Jin, *J. Control Release*, 2014, **174**, 126.
39 N. Schmidt, A. Mishra, G.H. Lai, G.C. Wong, *FEBS Lett.*, 2010, **584**, 1806.
40 V.P. Torchilin, *Adv. Drug Del. Rev.*, 2008, **60**, 548.
41 K.M. Wagstaff, D.A. Jans, *Eur. J. Pharmacol.*, 2009, **625**, 174.
42 B. Zhang, S. Mallapragada, *Acta Biomater.*, 2011, **7**, 1580.
43 H. Wajant, K. Pfizenmaier, P. Scheurich, *Apoptosis*, 2002, **7**, 449.
44 J. Dai, S. Zou, Y. Pei, D. Cheng, H. Ai, X. Shuai, *Biomaterials*, 2011, **32**, 1694.
45 Y.J. Chen, H.F. Liao, T.H. Tsai, S.Y. Wang, M.S. Shiao, *Int. J. Radiation Oncology Biol. Phys.*, 2005, **63**, 1252.

